High-Level Computational Study of the Stereoelectronic Effects of Substituents on Alkene Epoxidations with Peroxyformic Acid

Robert D. Bach,*[,1a] Mikhail N. Glukhovtsev,*[,1a] and Carlos Gonzalez[1b]

Contribution from the Department of Chemistry and Biochemistry, University of Delaware, Newark, Delaware 19716, and Physical and Chemical Properties Division of the National Institute of Standards and Technology, Gaithersburg, Maryland 20899

Received February 13, 1998. Revised Manuscript Received July 24, 1998

Abstract: The epoxidations of propene and isobutene with peroxyformic acid proceed by a concerted pathway via slightly unsymmetrical transition structures where the differences in the bond distances between the double-bond carbons and the spiro oxygen are only 0.021 and 0.044 Å at the QCISD/6-31G* level. In contrast, the more polarizable nature of the carbon−carbon double bond of α,β-unsaturated systems results in an unsymmetrical transition structure for the epoxidation of 1,3-butadiene with an order of magnitude difference in the carbon−oxygen bond distances of 0.305 Å at the QCISD/6-31G* level. A highly unsymmetrical transition structure has been also found at this level for the epoxidation of acrylonitrile. Notwithstanding the difference in the extent of asymmetry of the transition structures, both epoxidations of methyl-substituted alkenes and such α,β-unsaturated systems as 1,3-butadiene and acrylonitrile with peroxyformic acid follow a concerted asynchronous pathway. An unsymmetrical transition structure for 1,3-butadiene epoxidation and the concerted nature of the oxygen-transfer step are consistent with calculated kinetic isotope effects. The closeness of the barriers for propene and 1,3-butadiene epoxidations supports the conclusion that the reactions have similar mechanisms albeit they differ in the extent of asynchronous character of their transition structures. Methyl substitution leads to a decrease in the epoxidation barriers from 18.8 kcal/mol for ethylene to 13.7 kcal/mol for isobutene at the QCISD(T)/6-31G*//QCISD/6-31G* level. While the activation barrier for the epoxidation of 1,3-butadiene with peroxyformic acid (15.9 and 11.7 kcal/mol at the QCISD(T)/6-31G* and B3LYP/6-31G* levels, respectively) is close to that for propene epoxidation (16.0 and 12.0 kcal/mol at the QCISD(T) and B3LYP levels, respectively), the barrier for acrylonitrile epoxidation is higher (21.0 kcal/mol at the QCISD-(T)/6-31G* level). This increase in barrier height reflects the decreased nucleophilicity of double bonds bearing electron-withdrawing substituents. The energy differences between syn and anti configurations of the transition structures for the epoxidations of 1,3-butadiene and acrylonitrile with peroxyformic acid are very small (0.1−0.3 kcal/mol).

1. Introduction

Alkene epoxidation is a unique process that encompasses an impressive array of oxygen donors in both the industrial arena and under laboratory conditions. Early mechanistic studies on oxirane formation were experimental in nature,[2,3] while more recent attempts to describe the diverse transition structures for these oxidative processes have been largely of theoretical origin.[4−6] The key oxidants studied computationally have been peroxyformic acid (**1**) and dioxirane (**2**), as well as their isoelectronic nitrogen analogues, peroxynitrous acid (**3**) and oxaziridine (**4**), respectively.

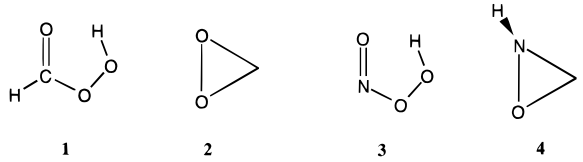

1 **2** **3** **4**

Alkene epoxidations can be classified formally as to the nature of the substrate and type of oxidant into four main groups: (i)

(1) (a) University of Delaware; WWW http://www.udel.edu/chem/bach and http://udel.edu/~mng; e-mail rbach@udel.edu and mng@udel.edu. (b) Physical and Chemical Properties Division, Building 221, Room A111, National Institute of Standards and Technology; e-mail cgonzale@email.nist.gov.

(2) (a) Hoveyda, A. H.; Evans, D. A.; Fu, G. C. *Chem. Rev.* **1993**, *93*, 1307. (b) Plesnicar, B. In *The Chemistry of Peroxides*; Patai, S., Ed.; Wiley: New York, 1983; p 521. (c) Swern, D. *Ibid.* 1971; Vol. 2, p 355. (d) Finn, M. G.; Sharpless, K. B. *Asymmetric Synth.* **1986**, *5*, 247. (e) Berti, G. *Topics in Stereochemistry*; Eliel. E. L., Allinger, N. L., Eds.; Wiley-Interscience: New York, 1973; Vol. 7, p 93. (f) Beak, P. *Acc. Chem. Res.* **1992**, *25*, 215.

(3) (a) Lynch, B. M.; Pausacker, K. H. *J. Chem. Soc.* **1955**, 1525. (b) Schwartz, N. N.; Blumbergs, J. H. *J. Org. Chem.* **1964**, *29*, 1976. (c) Vilka, M. *Bull. Soc. Chim. Fr.* **1959**, 1401. (d) Renolen, P.; Ugelstad, J. *J. Chim. Phys.* **1960**, *57*, 634. (e) House, H. O.; Ro, R. S. *J. Am. Chem. Soc.* **1958**, *80*, 2428. (f) Ogata, Y.; Tabushi, I. *J. Am. Chem. Soc.* **1961**, *83*, 3440, 3444. (g) Curci, R.; DiPrete, R. A.; Edwards, J. O.; Modena, G. *J. Org. Chem.* **1970**, *30*, 740. (h) Benassi, R.; Fiandri, L. G.; Taddei, F. *J. Org. Chem.* **1997**, *62*, 8018.

(4) (a) Cremer, D. In *The Chemistry of Peroxides*; Patai, S., Ed.; Wiley: New York, 1983; p 1. (b) Plesnicar, B.; Tasevski, M. A. *J. Am. Chem. Soc.* **1978**, *100*, 743. (c) Yamabe, S.; Kondou, C.; Minato, T. *J. Org. Chem.* **1996**, *61*, 616. (d) Singleton, D. A.; Merrigan, S. R.; Liu, J.; Houk, K. N. *J. Am. Chem. Soc.* **1996**, *118*, 3385. (e) Houk, K. N.; Condroski, K. R.; Pryor, W. A. *J. Am. Chem. Soc.* **1996**, *118*, 13002. (f) Houk, K. N.; Liu, J.; DeMello, N. C.; Condorski, K. R. *J. Am. Chem. Soc.* **1997**, *119*, 10147.

(5) (a) Bach, R. D.; Andrés, J. L.; Davis, F. A. *J. Org. Chem.* **1992**, *57*, 613. (b) Bach, R. D.; Owensby, A.; González, C.; Schlegel, H. B. *J. Am. Chem. Soc.* **1991**, *113*, 2338.

(6) (a) Bach, R. D.; Glukhovtsev, M. N.; Gonzalez, C.; Marquez, M.; Estévez, C. M.; Baboul, A. G.; Schlegel, H. B. *J. Phys. Chem. A* **1997**, *101*, 6092. (b) Baboul, A. G.; Schlegel, H. B.; Glukhovtsev, M. N.; Bach, R. D. *J. Comput. Chem.*, in press. (c) Bach, R. D.; Glukhovtsev, M. N.; Canepa, C. *J. Am. Chem. Soc.* **1998**, *120*, 775. (d) Bach, R. D.; Estévez, C. M.; Winter, J. E.; Glukhovtsev, M. N. *J. Am. Chem. Soc.* **1998**, *120*, 680.

S0002-7863(98)00495-8 CCC: $15.00
Published on Web 09/05/1998

symmetrical alkene (ethylene) and symmetrical oxidizing agents (peroxyformic acid (**1**), dioxirane (**2**), and peroxynitrous acid (**3**)), which can form a spiro-type transition structure where the plane of the oxidant is at 90° to the double bond with equivalent bonds between the carbons and the spiro oxygen; (ii) symmetrical alkene and unsymmetrical oxidant (oxaziridine (**4**)); (iii) unsymmetrical alkenes (propene, isobutene, and 1,3-butadiene) and symmetrical oxidant; (iv) unsymmetrical alkene and unsymmetrical oxidant. With the exception of case i, where a strictly symmetrical approach is predicted on the basis of electronic considerations, an asymmetrical approach to the alkene double bond should occur. These generalizations do not preclude a variety of other possible transition structures if a planar approach of the oxidizing reagent to the C−C bond axis is preferred on steric grounds.

Case i has been the most controversial in a recent series of papers.[4,6] The origin of this dilemma lies in the question of whether alkene epoxidation is a synchronous reaction with equal forming C−O bonds following a S_N2-type mechanism[5] or if the transition structure possesses some diradical character that can result in the development of multistep asynchronous processes such as that suggested recently for the MP2 potential energy surface.[4c] Intuitively, those oxidizing reagents such as **1**, **2**, and **3**, which retain their C_s symmetry in the transition structure (TS) for oxygen transfer to a symmetrically substituted double bond, should exhibit a symmetrical spiro-TS with essentially equal developing C−O bonds. Indeed, we have found that in epoxidation reactions with peroxy acids and peroxynitrous acid, where a 1,4-hydrogen shift attends the rate-limiting step and imposes planarity on the peracid, the oxidants do approach ethylene in a symmetrical fashion.[7] However, a multistep mechanism for the epoxidation of ethylene with peroxyformic acid that involves the formation of unsymmetrical transition structures and an intermediate has been recently proposed on the basis of MP2 calculations.[4c] In contrast to these MP2 calculations, geometry optimizations at the QCISD, CCSD, CASSCF, and DFT(B3LYP) levels of theory provide clear evidence for a single-step reaction via a symmetrical transition structure.[6a] The synchronous mechanism for the oxidation of simple alkenes with peroxyformic acid has also been confirmed in a combined theoretical and experimental study by Singleton et al. The reaction of peroxyformic acid with propene and the reaction of *m*-chloroperbenzoic acid with 1-pentene were used as theoretical and experimental models, respectively.[4d]

In the present study, we address the approach of the electrophilic oxygen in alkene epoxidations with an electronically symmetrical oxidant such as peroxyformic acid. It is conceivable that for case iii reactions substituents at the double-bond carbon can give rise to a highly unsymmetrical transition structure and to an asynchronous reaction pathway. To examine the effect of methyl substituents, we have considered epoxidations of ethylene (**5**), propene (**6**), isobutene (**7**), *trans*-2-butene (**8**), and *cis* -2-butene (**9**) with peroxyformic acid (**1**).

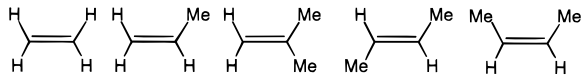

5 **6** **7** **8** **9**

We have also studied the role of mesomeric effects in the epoxidations of α,β-unsaturated systems which are exemplified by 1,3-butadiene (**10**) and acrylonitrile (**11**). The B3LYP/6-31G* calculations on these reactions have resulted in highly unsymmetrical transition structures. However, our experience[6] has shown that a highly correlated method is required to study the epoxidations of alkenes computationally, and therefore, we have carried out high-level calculations which include geometry optimizations for epoxidations of isobutene, 1,3-butadiene, and acrylonitrile with peroxyformic acid at the QCISD level that places considerable demands on computer resources. Could mesomeric effects in α,β-unsaturated systems cause a switch from a synchronous mechanism to an asynchronous mechanism, in contrast to simple alkenes, or is the B3LYP computational method artificially biased in favor of unsymmetrical transition structures as found for calculations[6c,7] of alkene epoxidations with peroxynitrous acid (**3**)? Since the previous data, including our own, have provided a mosaic presentation for this reaction mechanism, the present study attempts to draw a more homogeneous "portrait" of the overall reaction mechanism involving substrates more closely related to experiment.

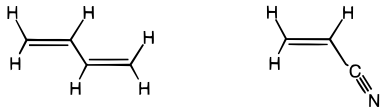

10 **11**

2. Computational Methods

Ab initio molecular orbital calculations[8] were performed with the GAUSSIAN 94 system of programs.[9] The Becke three-parameter hybrid functional[10a,11a] combined with the Lee, Yang, and Parr (LYP) correlation functional,[10b] denoted B3LYP,[11b] was employed in the calculations using density functional theory (DFT). The RB3LYP solutions for the all transition structures considered in this work are both singlet and triplet stable.[12] Geometries were optimized[13] at the B3LYP, MP2, and

(7) It was concluded recently on the basis of B3LYP/6-31G* calculations that the epoxidation of ethylene with peroxynitrous acid proceeds via an unsymmetrical transition structure.[4e,f] This observation is contrary to our basic precepts concerning the influence of electronic features on the transition structure and to the results of our QCISD calculations showing a symmetrical transition structure for this reaction.[6c] We have also observed that when a B3LYP solution to the wave function suffers from the RHF → UHF instability it typically results in an unsymmetrical transition structure.[6c,d] (d) The restricted B3LYP solution for the transition structure of the epoxidation of ethylene with peroxynitrous acid was reported[4f] to be stable. This conclusion was made because the UB3LYP/6-31G* calculations were found to lead to the same transition structure as those calculated at the RB3LYP level, indicating thereby that the RB3LYP solution for this transition structure is stable. In contrast, our calculations show that the triplet stability matrix is not positively defined and that wave function optimization gives a lower energy solution at the UB3LYP level.[6c]

(8) Hehre, W. J.; Radom, L.; Schleyer, P. v. R.; Pople, J. A. *Ab Initio Molecular Orbital Theory*; Wiley: New York, 1986.

(9) Frisch, M. J.; Trucks, G. W.; Schlegel, H. B.; Gill, P. M. W.; Johnson, B. G.; Robb, M. A.; Cheeseman, J. R.; Keith, T. A.; Peterson, G. A.; Montgomery, J. A.; Raghavachari, K.; Al-laham, M. A.; Zakrzewski, V. G.; Ortiz, J. V.; Foresman, J. B.; Cioslowski, J.; Stefanov, B. B.; Nanayakkara, A.; Challacombe, M.; Peng, C. Y.; Ayala, P. Y.; Wong, M. W.; Replogle, E. S.; Gomperts, R.; Andres, J. L.; Martin, R. L.; Fox, D. J.; Binkley, J. S.; DeFrees, D. J.; Baker, J.; Stewart, J. J. P.; Head-Gordon, M.; Gonzalez, C.; Pople, J. A. *GAUSSIAN-94*; Gaussian Inc.: Pittsburgh, PA, 1995.

(10) (a) Becke, A. D. *Phys. Rev. A* **1988**, *37*, 785. (b) Lee, C.; Yang, W.; Parr, R. G. *Phys. Rev.* **1988**, *B41*, 785.

(11) (a) Becke, A. D. *J. Chem. Phys.* **1993**, *98*, 5648. (b) Stevens, P. J.; Devlin, F. J.; Chablowski, C. F.; Frisch, M. J. *J. Phys. Chem.* **1994**, *80*, 11623.

(12) For the HF instabilities, see for example: (a) Seeger, R. R.; Pople, J. A. *J. Chem. Phys.* **1976**, *65*, 265. (b) Chambaud, G.; Levy, B.; Millie, P. *Theor. Chim. Acta* **1978**, *48*, 103. (c) Glukhovtsev, M. N.; Mestechkin, M. M.; Minkin, V. I.; Simkin, B. Ya. *Zh. Strukt. Khim. (USSR)* **1982**, *23*, 14. (d) Glukhovtsev, M. N.; Simkin, B. Ya.; Yudilevich, I. A. *Theor. Eksper. Khim. (USSR)* **1982**, *18*, 726. (e) Schlegel, H. B.; McDouall, J. J. W. In *Computational Advances in Organic Chemistry: Molecular Structure and Reactivity*; Ögretir, C., Csizmadia, I. G., Eds.; Kluwer: Dordrecht, The Netherlands, 1991; p 167. (f) Chen, W.; Schlegel, H. B. *J. Chem. Phys.* **1994**, *101*, 5957.

QCISD levels using the 6-31G* basis set.[8] The correlation-consistent p-VTZ basis set of Dunning[14] and the 6-311+G(3df,2p) basis set were used for geometry optimizations in calculations of epoxidations of butadiene and acrylonitrile with peroxyformic acid. The energies were refined by single-point calculations at the QCISD(T) and CCSD(T) levels[15] of theory using the 6-31G* and 6-311G** basis sets. The stationary points on the potential energy surfaces were characterized by calculations of vibrational frequencies at the B3LYP/6-31G* level. Zero point energies (ZPE) computed at the B3LYP/6-31G* level were scaled by 0.9806 according to Scott and Radom.[16] The reaction enthalpies were calculated using G2 theory.[17] Throughout the text, bond lengths are in angstroms and bond angles are in degrees.

3. Results and Discussion

Epoxidation of Methyl-Substituted Alkenes with Peroxyformic Acid: Isobutene. (a) Geometries of the Transition Structures. If the epoxidation of an alkyl-substituted alkene proceeds via an S_N2-type mechanism,[5] an electrophilic reagent should in principle approach the least substituted carbon atom in a Markovnikov-like fashion. For the epoxidation of propene with peroxyformic and peroxynitrous acids, both QCISD and CISD calculations result in a transition structure, where the electrophile is slightly skewed toward the least substituted carbon, with a small difference in the bond lengths between the spiro oxygen and the double-bond carbons.[6a,b]

A 1,1-disubstituted alkene like isobutene provides an ideal substrate to examine the electronic persuasion of an attacking electrophilic reagent. If the electrophile induces a positive center, it should exhibit a regiochemical preference for C_β reflecting the greater stability of the more highly substituted developing cationic center at C_α. Examination of the transition structure (TS-**12**) calculated at the B3LYP level (the RB3LYP/6-31G* solution for **12** is triplet stable; the lowest eigenvalue of the triplet stability matrix is 0.034 77 hartree)[12] shows that the O−C_1 (2.005 Å) and O−C_2 (2.195 Å) distances only slightly differ from each other (Figure 1). The QCISD/6-31G* geometry optimization confirms this result, and the transition structure becomes even more symmetrical (the O−C_1 and O−C_2 distances are 2.028 and 2.072 Å, respectively (Figure 1)). This demonstrates a general relationship between the B3LYP and QCISD geometries of the transition structures for alkene epoxidations: QCISD calculations lead to more symmetrical transition structures (Figures 1 and 2). In contrast to the B3LYP, CISD, and QCISD results, the MP2/6-31G* calculations lead to a anti-Markovnikov-type highly unsymmetrical transition structure with O−C_1 and O−C_2 distances of 2.192 and 1.899 Å, respectively (Figure 1, Table 1).[18] The dihedral angle between the plane of the peracid moiety and the axis of the C=C bond in all of the above transition structures is close to 90° (e.g., 89.8° and 89.7° in the transition structures of epoxidations of propene[6a] and isobutene (Figure 1), respectively).

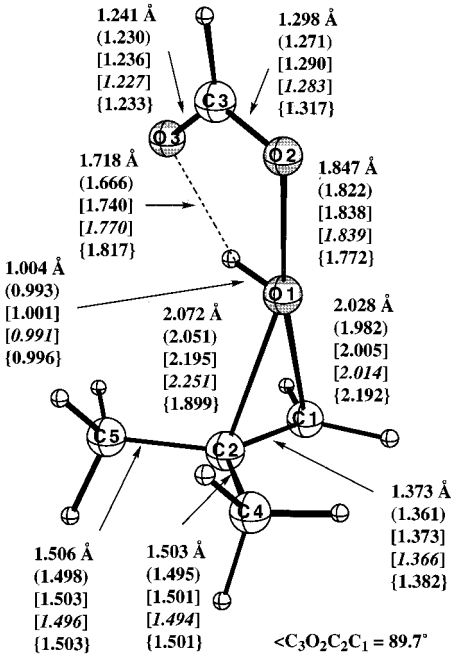

TS-12

Figure 1. Selected geometrical parameters of the transition structure (**12**) for the epoxidation of isobutene with peroxyformic acid calculated at the QCISD/6-31G*, CISD/6-31G* (in parentheses), B3LYP/6-31G* (in square brackets), B3LYP/6-311+G(3df,2p) (in italic in square brackets), and MP2/6-31G* (in curly brackets) levels. The calculated barrier heights are given in Table 2.

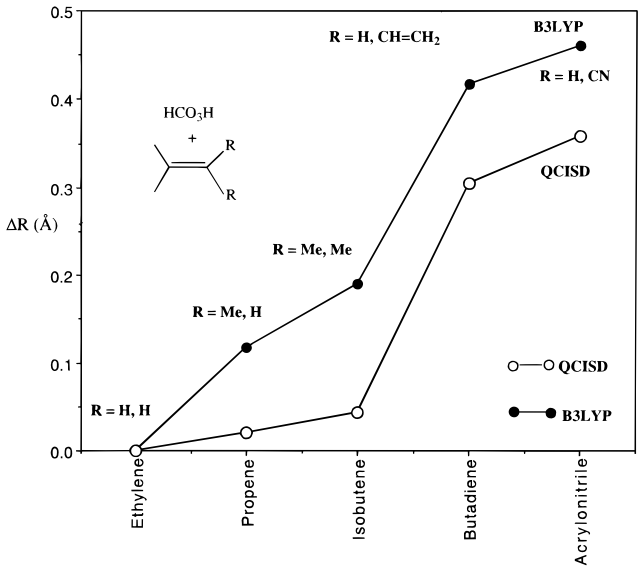

Figure 2. Plot of the differences in the lengths of the forming C−O bonds in alkenes oxidized with peroxyformic acid. The differences calculated at the B3LYP and QCISD levels are listed in Table 1.

As expected, 1,2-dimethyl-substituted ethylenes, **8** and **9**, demonstrate much less difference in the O−C_1 and O−C_2 distances in their transition structures with peroxyformic acid[6a] when compared with those in the TS for the 2-methylpropene (isobutene) (Table 1). The difference in the C−O bonds (2.104 and 2.125 Å) of the developing epoxide in the peroxyformic acid epoxidation of allyl alcohol computed at the B3LYP/6-311G(d,p) level (0.021 Å)[6d] is also less than that for propene.

(b) Activation Barriers. The activation barriers calculated at the B3LYP and MP2 levels are close to each other (10.8 and

(13) (a) Schlegel, H. B. *J. Comput. Chem.* **1982**, *3*, 214. (b) Schlegel, H. B. *Adv. Chem. Phys.* **1987**, *67*, 249. (c) Schlegel, H. B. In *Modern Electronic Structure Theory*; Yarkony, D. R., Ed.; World Scientific: Singapore, 1995; p 459.

(14) Dunning, T. H. *J. Chem. Phys.* **1989**, *90*, 1007.

(15) (a) Pople, J. A.; Head-Gordon, M.; Raghavachari, K. *J. Chem. Phys.* **1987**, *87*, 5968. (b) Bartlett, R. J.; Purvis, G. D. *Int. J. Quantum Chem.* **1978**, *14*, 516. (c) Bartlett, R. J. *Annu. Rev. Phys. Chem.* **1981**, *32*, 359.

(16) Scott, A. P.; Radom, L. *J. Phys. Chem.* **1996**, *100*, 16502.

(17) Curtiss, L. A.; Raghavachari, K.; Trucks, G. W.; Pople, J. A. *J. Chem. Phys.* **1991**, *94*, 7221.

(18) Oxygen attack at the more highly substituted carbon is apparently an artifact of the MP2 method. While the B3LYP and QCISD calculations show that methyl substituents lead to a monotonic increase of the difference in the O−C_1 and O−C_2 distances in transition structures for epoxidations, from ethylene **5** to propene **6** to isobutene **7**, the MP2 data do not provide a systematic trend (Table 1).

Table 1. Differences (Å) in the $O-C_1$ and $O-C_2$ Distances of Transition Structures for the Epoxidations of Alkenes with Peroxyformic Acid

substrate	ΔR (MP2/6-31G*)	ΔR (B3LYP/6-31G*)	ΔR (QCISD/6-31G*)
ethylene	0.458	0.0	0.0
propene	0.537[a]	0.117	0.021
isobutene	−0.293[b]	0.190[c]	0.044[d]
cis-2-butene		0.001	
trans-2-butene		0.034	
1,3-butadiene (TS-**13a**)	0.519	0.417[e]	0.305[f]
acrylonitrile (TS-**14b**)	0.465	0.460[g]	0.358

[a] Two transition structures were found at the MP2/6-31G* level. The difference in the CO distances is given for a Markovnikov-type structure. While Markovnikov-type transition structures (albeit much more symmetrical) were found at the B3LYP and QCISD levels, this MP2 TS is 0.2 kcal/mol higher than an anti-Markovnikov TS (for which the distance difference is −0.363 Å). [b] The MP2 transition structure exhibits a regiochemical preference for C_1, in contrast to the B3LYP and QCISD results (Figure 1). [c] 0.237 Å at the B3LYP/6-311+G(3df,2p) level. [d] 0.069 Å at the CISD/6-31G* level. [e] 0.424 Å at the B3LYP/6-311+G(3df,2p) level. [f] 0.209 Å at the CISD/6-31G* level. [g] 0.439 Å at the B3LYP/6-311+G(3df,2p) level.

10.6 kcal/mol, respectively, Table 2) despite the different geometries of the transition structure (Figure 1). The B3LYP/6-31G* barrier for the epoxidation of isobutene is 2.9 kcal/mol lower than that calculated at the QCISD(T)/6-31G* level (Table 2, Figure 3). However, at the B3LYP/6-311+G(3df,2p)//B3LYP/6-311G(3df,2p) level, the barrier (13.1 kcal/mol) increases as the flexibility of the basis set is increased and is closer to the QCISD(T)/6-31G*//QCISD/6-31G* value (13.7 kcal/mol). An expansion of the basis set also results in a modest increase in barrier when the QCISD method is applied. As seen from Table 2, 1,1-dimethyl substitution leads to a decrease in the barrier heights from 18.8 kcal/mol for ethylene to 13.7 kcal/mol for isobutene at the QCISD(T)/6-31G* level. 1,2-Dimethyl substitution results in almost the same barrier (10.0 and 10.4 kcal/mol for *cis*-2-butene (**9**) and *trans*-2-butene (**8**) at the B3LYP/6-31G* level, respectively)[6a] as that for isobutene (**7**) in good agreement with experiment.[2a,16]

The barrier for the epoxidation of isobutene calculated at the QCISD/6-31G* level using the CISD/6-31G*-optimized geometries (14.5 kcal/mol, Table 2) is reasonably close to the QCISD(T)/6-31G*//QCISD/6-31G* barrier (13.7 kcal/mol) (Figure 3). Similar trends are observed for the epoxidation of 1,3-butadiene (Table 2). This suggests the possibility of using the CISD geometry optimization since it is less demanding of computer resourses than QCISD calculations. It is interesting to note that, although the CISD optimization gives shorter O−O and C−O bond distances, the barriers are increased somewhat. A comparison of the barriers for epoxidations of ethylene, propene, isobutene, 1,3-butadiene, and acrylonitrile with peroxyformic acid calculated at the QCISD(T)/6-31G*//B3LYP/6-31G* level with the QCISD(T)/6-31G*//QCISD barriers (Table 2, Figure 3) leads to the conclusion[6a] that using B3LYP geometries in the QCISD(T) calculations can be cost effective and, at the same time, provide a reliable computational approach to study epoxidations of alkenes with peroxyformic acid.

Epoxidation of α,β-Unsaturated Systems: 1,3-Butadiene and Acrylonitrile. (a) Transition Structures and Barrier Heights. The potential energy surface for the approach of peroxyformic acid to a conjugated diene is much steeper than that observed with a simple alkene. There are two types of transition structures for epoxidations of 1,3-butadiene and acrylonitrile, which differ by a syn or anti orientation of the peroxyformic moiety with respect to the vinyl or cyano substitutent. These syn and anti transition structures for epoxidation of 1,3-butadiene (TS-**13a,b**) and acrylonitrile (TS-**14a,b**) are very close each to other in energy (Table 2) and geometry (Figure 4). Therefore, we have performed our highest level geometry optimizations (QCISD/6-31G*) only for the lowest energy configurations, which are the syn transition structure **13a** for 1,3-butadiene and the anti transition structure **14b** for acrylonitrile (Table 2).

For 1,3-butadiene, not only MP2/6-31G* calculations but also the CISD/6-31G*, QCISD/6-31G*, B3LYP/6-311+G(3df,2p), and B3LYP/6-31G* levels of theory lead to highly unsymmetrical transition structures with the C−O bonds formed to very different extents (only B3LYP and MP2 calculations were carried out for *anti*-TS-**13b**).[19] All four methods indicate a transition structure (TS-**13a** or TS-**13b**) that resembles a Michael-type nucleophilic addition to a conjugated alkene (Figure 4).[20] Furthermore, the distances between the spiro oxygen and the double-bond carbons in TS-**13a** calculated by all of these methods are similar, in contrast to the transition structure geometries calculated for epoxidations of nonconjugated alkenes (Figure 2). For example, the differences between the O_1-C_1 and O_1-C_2 bond distances, which is a measure of asynchronous character, are 0.305, 0.417, and 0.519 Å in 1,3-butadiene TS-**13a** at the QCISD, B3LYP, and MP2/6-31G* levels, respectively (Table 1). This difference is 0.424 Å at the B3LYP/6-311+G(3df,2p) level. The CISD/6-31G* optimization results in a smaller difference in these bond distances (0.209 Å). A comparison of the B3LYP, QCISD, CISD, and MP2 computational data with the experimental results[21] allows us to conclude that MP2 calculations are capable of providing geometrically correct transition structures for epoxidations of α,β-unsaturated systems.[20] In general, we have found that the MP2 level also affords adequate geometries for transition structures for the oxidation of amines, phosphines and sulfides.[6]

While the *anti*-1,3-butadiene TS-**13b** is 0.7 kcal/mol lower in energy at the MP2/6-31G* level, it is slightly higher than *syn*-TS-**13a** at the MP4/6-31G*, B3LYP/6-31G*, and QCISD(T)/6-31G*//B3LYP/6-31G* levels of theory (Table 2). The QCISD(T)/6-31G*//QCISD/6-31G* barrier for the formation of the epoxide of 1,3-butadiene is predicted to be 15.9 kcal/mol (TS-**13a**, Table 2). The B3LYP barrier height[22] is 4.2 kcal/mol lower, whereas the QCISD(T)/6-31G* barrier calculated using the B3LYP/6-31G* geometries (15.7 kcal/mol) is close

(19) (a) Swern, D. J. *J. Am. Chem. Soc.* **1947**, *69*, 1692. (b) The relative rates of epoxidation of ethylene, propylene, styrene, isobutene, and 2-butene with peracetic acid are 1, 22, 59, 484, and 489, respectively.[16a.]

(20) (a) While the MP2 method is apparently biased in favor of unsymmetrical transition structures for alkene epoxidation,[6a] transition structures for epoxidations of such α,β-unsaturated systems as 1,3-butadiene and acrylonitrile are highly unsymmetrical and the MP2 method gives qualitatively correct structural types for these transition structures. (b) The B3LYP/6-31G* data on the epoxidation of butadiene with peroxyformic acid were reported by Professor K. N. Houk[4d] when this paper was in preparation.

(21) Hanzlik, R. P.; Shearer, G. O. *J. Am. Chem. Soc.* **1975**, *106*, 1401.

(22) (a) The T_1 test[22b] for transition structure (TS-**13a**) at the CCSD(T)/6-31G* level ($T_1 = 0.026$) is slightly above the threshold of 0.02 that was suggested using computational data on Be_n and Mg_n clusters (at their equilibrium structures) prompting us to examine the wave function stability of the TS in question. The possibility of biradical character in transition structures for epoxidations of isobutene, butadiene, and acrylonitrile is ruled out since the RB3LYP/6-31G* solutions for all three transition structures are both *singlet and triplet stable* (the lowest eigenvalues of the triplet instability matrices are 0.03477 (**12**), 0.01305 (**13a**), and 0.00317 (**14b**) hartree, respectively). Examining the triplet instability[12] is a well-documented test for the possibility of diradical character (see ref 6a and publications cited there). Therefore, the IRC calculations using the B3LYP/6-31G* which are reported in this paper are also reliable. (b) Lee, T. J.; Taylor, P. R. *Int. J. Quantum Chem. Symp.* **1989**, *23*, 199.

Table 2. Activation Barriers and Reaction Enthalpy Changes (kcal/mol) for the Epoxidation of Alkenes with Peroxyformic Acid Calculated at Various Computational Levels[a]

substrate	$\Delta E^{\ddagger}$ (MP2/6-31G*//MP2/6-31G*)	$\Delta E^{\ddagger}$ (MP4/6-31G*//MP2/6-31G*)	$\Delta E^{\ddagger}$ (B3LYP/6-31G*)	$\Delta E^{\ddagger}$ (QCISD(T)/6-31G*//B3LYP/6-31G*)	$\Delta E^{\ddagger}$ (QCISD(T)/6-31G*//QCISD/6-31G*)	ΔH (0 K) G2[j]
ethylene	16.5	16.3	14.1 (14.6)[b]	18.7	18.8	−47.7 (−48.3)[k]
propene	13.8	-	12.0	15.9	16.0	−50.2(−50.0)[k]
isobutene	11.2	10.6 (10.4)[b]	10.8 (10.9)[c,d]	13.8	13.7 (14.5)[e]	−52.0 (−52.4)[k]
trans−2-butene	10.9	10.4	10.4 (10.8)[c,f]			
1,3-butadiene *syn*-TS	12.7	12.4 (12.0)[b]	11.7 (12.2)[c,g]	15.7	15.9 (17.1)[e,h]	−46.9 (−47.3)[k]
1,3-butadiene *anti*-TS	12.0	12.5 (12.2)[b]	11.8	15.9		
acrylonitrile *syn*-TS	16.4	17.1	17.4			
acrylonitrile *anti*-TS	16.2	16.8 (16.3)[b]	17.3[i]	20.8	21.0	−44.4 (−44.8)[k]

[a] The barrier heights are relative to the isolated reactants. The barriers for ethylene and propene epoxidations are given for the sake of comparison. [b] The MP4/6-31G*//B3LYP/6-31G* barrier is given in parentheses. [c] The barriers calculated at the B3LYP/6-31+G* level are given in parentheses. [d] 13.1 kcal/mol at the B3LYP/6-311+G(3df,2p)//B3LYP/6-311+G(3df,2p) level. [e] The QCISD(T)/6-31G*//CISD/6-31G* values are shown in parentheses. [f] The B3LYP/6-31G* barrier for the epoxidation of *cis*-2-butene is 10.0 kcal/mol. [g] The barriers calculated at the B3LYP/cc-pVTZ//B3LYP/cc-pVTZ and B3LYP/6-311+G(3df,2p)//B3LYP/6-311+G(3df,2p) levels are 14.6 and 14.5 kcal/mol, respectively. [h] The QCISD(T)/6-311G**//QCISD/6-31G* and CCSD(T)/6-31G*//QCISD/6-31G* barrier heights are 17.3 and 16.3 kcal/mol, respectively. [i] 20.5 kcal/mol at the B3LYP/6-311+G(3df,2p)//B3LYP/6-311+G(3df,2p) level. [j] The G2-calculated energies of the reactants and products are given as Supporting Information (Table 1S). The G2 energies of 1,3-butadiene and formic acid were taken from refs 24a and 24b, respectively. [k] G2 reaction enthalpies at 298 K are given in parentheses.

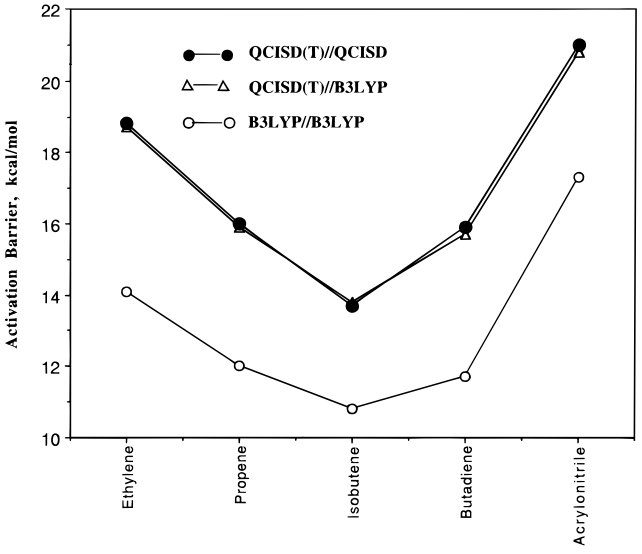

Figure 3. Plot of the barrier heights for the alkene epoxidations with peroxyformic acid calculated at various levels of theory. The calculated barrier values are given in Table 2.

to that found at the QCISD(T)/6-31G* level (Figure 3). At the MP4SDTQ/6-31G*//MP2/6-31G* level, the difference between computed classical barriers for ethylene and 1,3-butadiene is 3.9 kcal/mol. This energy difference is reduced to 2.9 and 2.4 kcal/mol at the QCISD(T)/6-31G*//QCISD/6-31G* and B3LYP/6-31G*//B3LYP/6-31G* levels of theory, respectively. These data suggest that the problem with MP2 geometries is not extended to conjugated alkenes with more polarizable double bonds. The increased MP4//MP2/6-31G* barrier for acrylonitrile epoxidation (16.8 kcal/mol) with respect to that for the epoxidation of 1,3-butadiene (12.4 kcal/mol at the same level of theory) reflects the decreased nucleophilicity of double bonds bearing electron-withdrawing substituents. The corresponding barriers calculated at the QCISD(T)/6-31G*//QCISD/6-31G* level are 21.0 and 15.9 kcal/mol, respectively (Table 2). A basis set extension from the 6-31G* to cc-pVTZ and the 6-311+G(3df,2p) basis sets results in a small increase in the B3LYP barriers for the epoxidation of butadiene. The calculated barrier values (14.6 and 14.5 kcal/mol, respectively) are close to the QCISD(T)/6-31G*//QCISD/6-31G* and QCISD(T)/6-31G*//B3LYP/6-31G* values (15.9 and 15.7 kcal/mol, respectively). The calculations at the QCISD(T)/6-311G**//QCISD/6-31G* level of theory led to a barrier of 17.3 kcal/mol. The CCSD(T)/6-31G*//QCISD/6-31G* calculated barrier (16.3 kcal/mol) is also close to the QCISD(T)/6-31G* value.

The approach of the electrophilic oxygen in the TS for the epoxidation of acrylonitrile with peroxyformic acid (TS-**14a,b**, Figure 4) at the MP2 level closely resembles that for 1,3-butadiene. The anti configuration of the transition structure (**14b**) is lower in energy than the syn TS (**14a**), albeit the energy difference is very small (0.1 and 0.3 kcal/mol at the B3LYP/6-31G* and MP4/6-31G*//MP2/6-31G* levels, respectively, Table 2). An unsymmetrical approach of the electrophilic oxygen to the double bond (the $C_1-O_{(spiro)}$ and $C_2-O_{(spiro)}$ distances in **14b** are 1.806 and 2.164 Å at the QCISD/6-31G*, respectively; Figure 4), reflecting the electronic effect of the mesomeric substituent. The difference in this distance is 0.439 Å at the B3LYP/6-311+G(3df,2p) level (Table 1). The dihedral angles between the peracid moiety and the C−C bond axis ($\angle O_3C_3C_2C_1$) in TS-**13a** and TS-**14b** are 101.0° and 109.7°, respectively, indicating a deviation from an ideal (90°) spiro orientation as a consequence of the polarizability of the multiply bonded substitutents on the double bond. The activation barrier for the epoxidation of acrylonitrile with peroxyformic acid is about 5−6 kcal/mol higher than that for the epoxidation of 1,3-butadiene (Table 2, Figure 3).

Notwithstanding the unsymmetrical character of the transition structures both for the epoxidation of 1,3-butadiene and acrylonitrile, these transition structures correspond to a concerted reaction pathway although the C−O bond formation is asynchronous. An animation of the B3LYP/6-31G* vibration mode corresponding to the negative eigenvalue of the Hessian for the transition structure of 1,3-butadiene and peroxyformic acid **13a** shows the transfer of the oxygen to C_1 accompanied by O_1-O_2 bond elongation with $sp^2 \rightarrow sp^3$ rehybridization at the terminal carbon as it moves out of the plane toward the electrophilic oxygen. There is comparatively little motion of C_2 in **13a,** and no O−H bond motion is observed. By contrast, in the transition structure for the epoxidation of isobutene with peroxyformic acid (TS-**12**) (Figure 1), the oxygen atom approaches the center of the C=C bond and both C_1 and C_2 carbons experience $sp^2 \rightarrow sp^3$ rehybridization with the lighter hydrogen atoms at C_1, showing more motion than the two methyl groups. This type of S_N2 attack by the π-bond along the O−O bond axis is consistent with the endocyclic restriction test developed by Beak to probe the geometry at heteroatoms under nucleophilic attack.[2f]

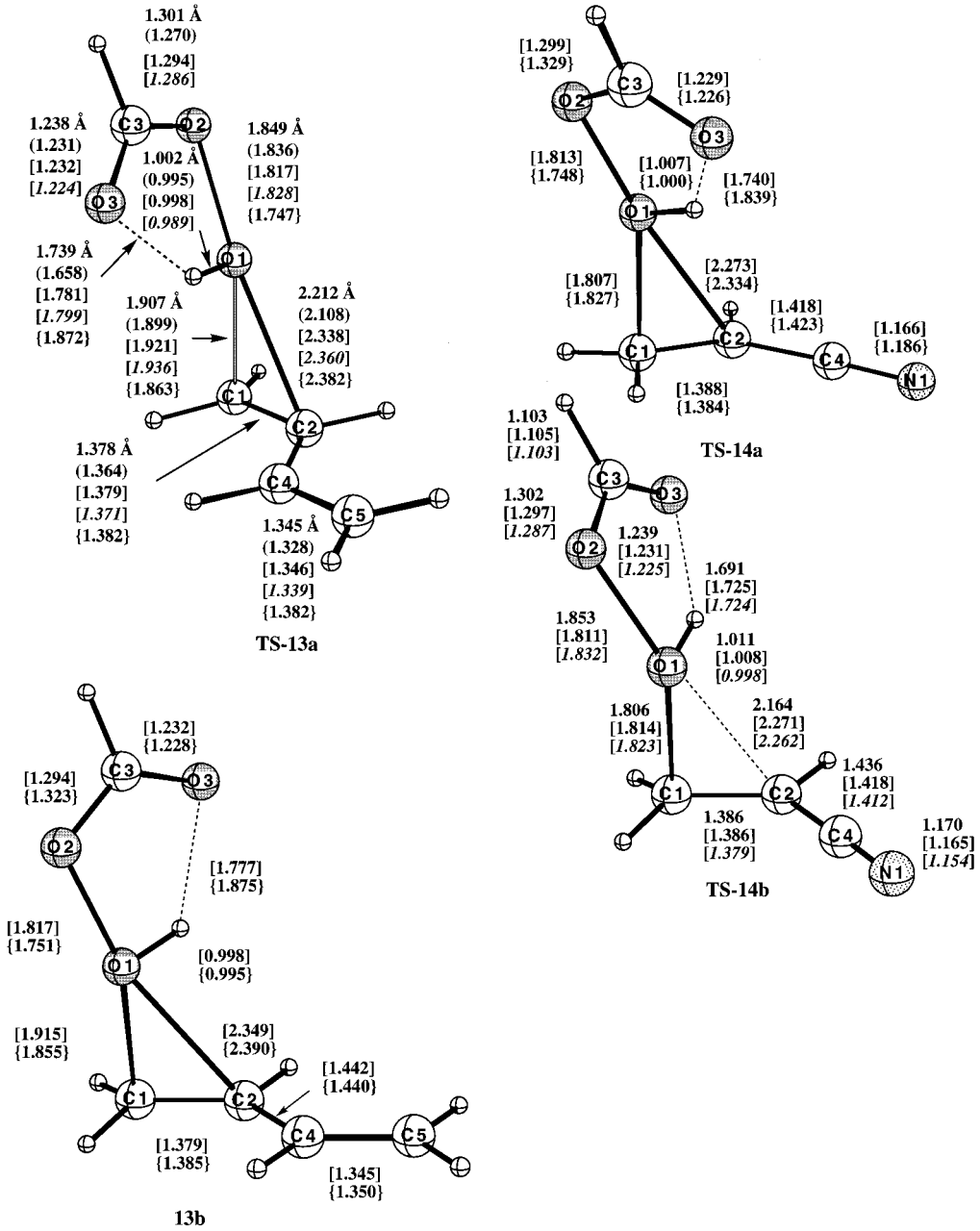

Figure 4. Selected geometrical parameters of the transition structures for the epoxidation of 1,3-butadiene (**13a**,**b**) and acrylonitrile (**14a**,**b**) with peroxyformic acid calculated at the QCISD/6-31G*, CISD/6-31G* (in parentheses), B3LYP/6-31G* (in square brackets), and MP2/6-31G* (in curly brackets) levels. The B3LYP/6-311+G(3df,2p) values for **13a** and **14b** are given in italic in square brackets.

We also calculated the reaction path followed by intrinsic reaction coordinate (IRC).[23] These calculations at the B3LYP/6-31G* level led to pre- and postreaction complexes whose geometries (**15** and **16**) were then optimized separately and confirmed with calculating their Hessians to be minima. A structure of the prereaction complex (**15**) for the epoxidation of butadiene with peroxyformic acid calculated at the B3LYP/6-31G* level demonstrates an almost symmetrical approach of the carboxyl hydrogen in the peroxyformic moiety to the center of the C=C bond of 1,3-butadiene (slightly skewed to the terminal carbon with a difference in the −OOH hydrogen and C_1/C_2 distances of 0.155 Å (Figure 5)). The peroxy oxygen is located almost equally from the C_1 and C_2 atoms (3.240 and 3.356 Å, respectively). This difference in the peroxy oxygen C_1/C_2 distances is only 0.116 Å and increases to 0.417 Å in the transition structure (**13a**). In the postreaction complex **16** this difference in the C−O bond distances is only 0.020 Å (Figure 5). The complexation energies for **15** and **16** calculated at the B3LYP/6-31G*+ZPE(B3LYP/6-31G*) level are 2.7 and 10.7 kcal/mol with respect to the reactants and products, respectively. The larger complexation energy of **16** can be a result of the relatively short hydrogen bond between the oxirane oxygen and carboxyl hydrogen separated by only 1.755 Å (Figure 5).

The reaction enthalpy changes could be expected to be proportional to the corresponding activation barriers. The G2[17]-calculated reaction enthalpies for epoxidations of butadiene and acrylonitrile confirm this suggestion (Table 2). However, such a relationship appears to hold only for similar structural types of alkenes as shown by a comparison with the reaction enthalpy and activation energy for the epoxidation of ethylene. While this reaction is more exothermic than the epoxidation of 1,3-butadiene, its activation barrier (18.8 kcal/mol) is higher than that for butadiene (15.9 kcal/mol). For ethylene, propene, and

(23) Gonzalez, C.; Schlegel, H. B. *J. Chem. Phys.* **1989**, *90*, 2154.

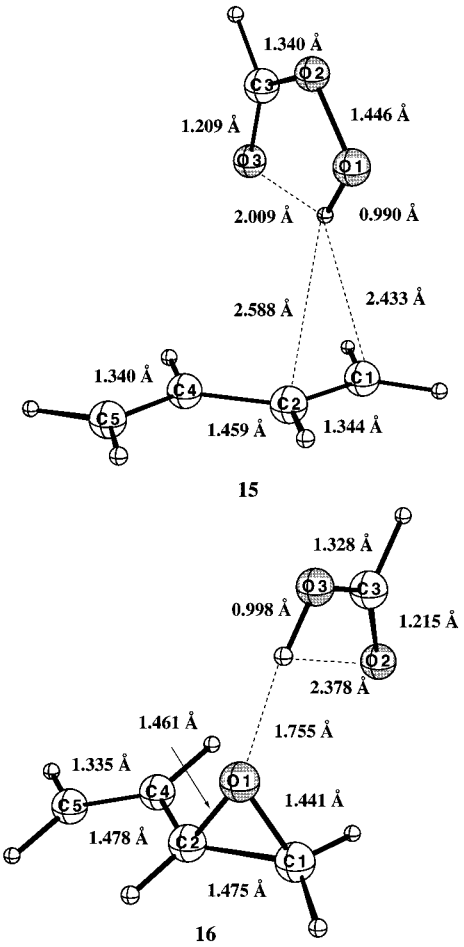

Figure 5. Selected geometrical parameters of the pre- and postreaction complexes for the epoxidation of 1,3-butadiene with peroxyformic acid (**15** and **16**, respectively) calculated at the B3LYP/6-31G* level.

isobutene, the more exothermic the oxidations, the lower the activation barriers (Table 2).

The closeness of the barriers for propene and 1,3-butadiene epoxidations supports the conclusion that both reactions have similar mechanisms albeit they differ in the asynchronous character of their transition structures. The Wiberg bond indexes[25] calculated for the $C_1-O_{(spiro)}$ and $C_2-O_{(spiro)}$ distances in TS-**13b** using natural population analysis[26] are 0.392 and 0.184, respectively, at the B3LYP/6-31G* level. Furthermore, supporting evidence for the concerted nature of the oxygen-transfer step comes from consideration of inverse kinetic isotope effects in the epoxidation of 1,3-butadiene.

(b) Inverse Kinetic Isotope Effects. Experimentally determined kinetic isotope effects (KIEs) are one of the few available experimental tools that can probe the geometry of a transition state.[27] An assessment of the accuracy of transition state geometries also remains a goal of the theoretical chemist. Theoretically calculated KIEs have been used to predict the nature of a transition structure.[28] We have recently also shown that secondary KIEs calculated at the MP2 level for alkene-forming elimination reactions are in excellent agreement with experiment.[29]

Diastereotopically distinct isotopic substitution in 1,3-butadiene should also provide an independent test of the ability of high-level ab initio calculations to accurately predict a transition structure for epoxidation. Significant secondary isotope effects should be anticipated in an electrophilic addition to an alkene when there is a discernible change in hybridization from sp^2 to sp^3 in the transition state at the isotopically substituted position.[30] In a classic experiment, Hanzlik[21] used this concept to define the geometry of the transition state and the timing of the bonding changes in the epoxidation of a specifically deuterated *p*-phenylstyrene with *m*-chlorobenzoic acid (TS-**17**, Figure 6). Since the sp^2 carbon atoms become more sp^3-like in the resulting epoxide, the energy of activation for an $sp^2 \rightarrow sp^3$ change in hybridization is *lower* for a deuterium-substituted double bond and the KIE is inverse with $k_H/k_D < 1.0$. The failure to observe an isotope effect for the arylethene-α-d_2 ($k_H/k_D = 0.99$) and the observation of a significant KIE for the β,β-d_2-substituted styrene ($k_H/k_D = 0.82$) suggested that only the β-carbon had undergone a discernible change in its hybridization from sp^2 to sp^3. These data led Hanzlik to the generalization that all transition structures for epoxidation resemble TS-**17**, where only one C−O bond of the oxirane product is formed and that the unsymmetrical nature of the TS was not simply a consequence of a monosubstituted alkene.

The classical barrier and harmonic frequency (MP2/6-31G*) were used to calculate the reaction rate constants at 298 K using canonical transition-state theory.[31] The rate constants with and without Wigner[32a] and Bell[32b] tunneling corrections[32] gave comparable KIE results (Table 3), indicating that the kinetics are not measurably affected by tunneling at room temperature. The relatively high activation barriers and the small tunneling corrections at 298 K suggested that the use of the more accurate variational transition theory is not necessary for this particular KIE analysis.[33]

We have used the MP2/6-31G* level of theory to compute vibrational frequencies and zero-point energies. These frequencies were used unscaled to compute theoretical secondary isotope effects at 298 K. For the six substrates examined thus

(24) (a) Glukhovtsev, M. N.; Laiter, S.; Pross, A. *J. Phys. Chem.* **1995**, *99*, 6828. (b) Bach, R. D.; Ayala, P. Y.; Schlegel, H. B. *J. Am. Chem. Soc.* **1996**, *118*, 12758.

(25) For applications of Wiberg bond indexes in analysis of various bonding patterns, see for example: Glukhovtsev, M. N.; Schleyer, P. v. R. *Chem. Phys. Lett.* **1992**, *198*, 547.

(26) For natural population analysis, see: (a) Reed, A. R.; Weinstock, R. B.; Weinhold, F. *J. Chem. Phys.* **1985**, *83*, 735. (b) Reed, A. E.; Curtiss, L.A.; Weinhold, F. *Chem. Rev.* **1988**, *88*, 899. (c) Weinhold, F.; Carpenter, J. E. In: *The Structure of Small Molecules and Ions*; Naaman, R., Vager, Z., Eds.; Plenum Press: New York, 1988; p 227. (d) Reed, A. E.; Weinhold, F. *Isr. J. Chem.* **1991**, *31*, 277.

(27) (a) Shiner, V. J., Jr. In *Isotope Effects in Chemical Reactions*; Collins, C. J., Bowman, N. S., Eds.; Van Nostrand Reinhold: New York, 1970. (b) Melander, L.; Saunders: W. H., Jr. *Reaction Rates of Isotopic Molecules*; Wiley: New York, 1980. (c) Gajewski, J. J. *Isotopes in Organic Chemistry*; Buncel, E., Lee, C. C., Eds.; Elsevier: Amsterdam, 1987; Vol. 7.

(28) (a) Dewar, M. J. S.; Ford, G. P. *J. Am. Chem. Soc.* **1977**, *99*, 8343. (b) Saunders, M.; Lidig, K. E.; Wolfsberg, M. *Ibid.* **1989**, *111*, 8989. (c) Chantranupong, L.; Wildman, T. A. *Ibid.* **1990**, *112*, 4151. (d) Wolfe, S.; Hoz, S.; Kim, C.-K.; Yang, K. *Ibid.* **1990**, *112*, 4186. (e) Axelsson, B. S.; Matsson, O.; Langstrom, B. *Ibid.* **1990**, *112*, 6661. (f) Houk, K. N.; Gustafson, S. M.; Black, K. A. *Ibid* **1992**, *114*, 8565.

(29) Bach, R. D.; Gonzalez, C.; Andrés, J. L.; Schlegel, H. B. *J. Org. Chem.* **1995**, *60*, 14653.

(30) (a) Streitwieser, A., Jr.; Jagow, R. H.; Fahey, R. C.; Suzuki, S. *J. Am. Chem. Soc.* **1958**, *80*, 2326. (b) Poirer, R. D.; Wang, Y.; Westaway, K. C. *J. Am. Chem. Soc.* **1994**, *116*, 2526.

(31) (a) Steinfeld, J. I.; Francisco, J. S.; Hase, W. L. *Chemical Kinetics and Dynamics*; Prentice Hall: Englewood Cliffs, NJ, 1989. (b) Carm, D. J.; McCarty, J. E. *J. Am. Chem. Soc.* **1954**, *76*, 5740. (c) Cope, A. C.; LeBel, N. A. *Ibid.* **1960**, *82*, 4656. (d) Saunders: W. H., Jr.; Cockerill, A. F. *Mechanisms of Elimination Reactions*; Wiley: New York, 1973.

(32) (a) Wigner, E. P. *A. Phys. Chem.* **1932**, *B19*, 203. (b) Bell, R. P. *The Proton in Chemistry*, 2nd ed.; Chapman and Hall: London, 1973, Chapter 12.

(33) (a) Skodje, R. T.; Truhlar, D. G.; Garret, B. C. *J. Chem. Phys* **1982**, *77*, 5955. (b) Steckler, R.; Dykema, K. J.; Brown, F. B.; Hancock, G. C.; Truhlar, D. G.; Valeneich, J., Jr. *Ibid.* **1987** *87*, 7024.

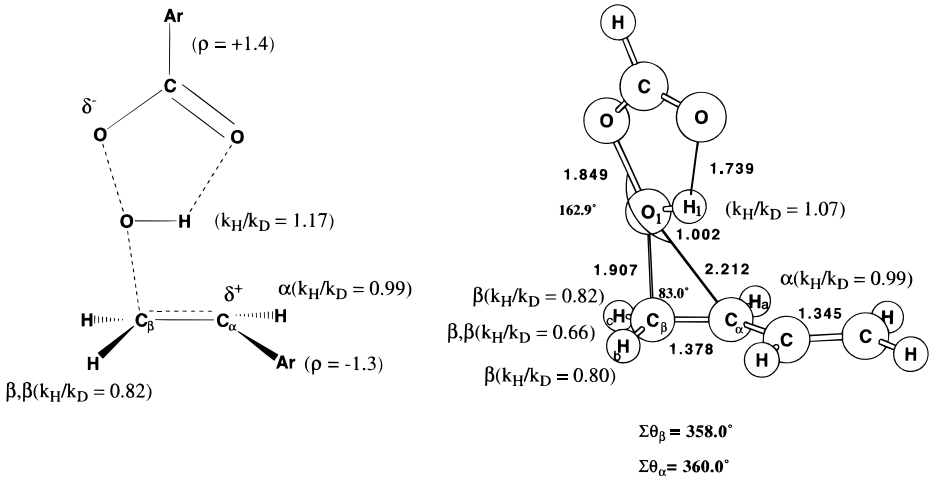

Figure 6. Proposed transition structure (TS-**17**) for epoxidation of an aryl substituted styrene and transition structure **13a** for epoxidation of 1,3-butadiene (calculated at the QCISD/6-31G* level). The theoretical isotope effects were calculated at the MP2/6-31G* level using the Bell tunneling correction.

Table 3. Calculated Primary and Secondary Kinetic Isotope Efeects for the Oxidation of 1,3-Butadiene with Peroxyformic Acid (298 K) and Wigner and Bell Tunneling Corrections[a]

type		Wigner	Bell
primary (O_1-H1)	1.0760	1.0749	1.0747
secondary (C_α-D)	0.9859	0.9858	0.9858
secondary C_β-D, cis)	0.7075	0.7974	0.7975
secondary (C_β-D, trans)		0.8215	0.8216
secondary (C_β-D_2)	0.6551	1.0066	0.6556
heavy atom (C^{14}, C_α)	1.0062		1.0067
heavy atom (C^{14}, C_β)	1.0464	1.0577	1.0622

[a] The KIE values are computed using an unscaled harmonic frequency at the MP2/6-31G* level.

far, both the magnitude and trend shown for the activation barriers (MP4SDTQ/6-31G*//MP2/6-31G*) in the gas phase are in excellent agreement with experiment. This is perhaps not too surprising since peroxy acid epoxidation proceeds best in nonpolar solvents.[2] The calculated KIE for deuterium substitution at the α-carbon in TS-**13a** (H_a) is 0.99, in excellent agreement with the experimental value for an aryl-substituted styrene. The KIE for diastereotopically distinct hydrogen (H_b) on the *β*-carbon cis to the vinyl substituent is 0.80, while that for H_c is predicted to be 0.82. The calculated *β*,*β*-d_2 KIE is 0.66 for this transition structure with H_c, reflecting the extensive rehybridization at C_β. Consistent with these data the sum of the three bond angles about C_α is 359.8°, indicating a planar sp^2 carbon atom, while the angle at C_β is 355.7° (MP2/6-31G* geometry; this difference is smaller at the QCISD/6-31G* geometry (Figure 6)). The sum of these three angles at an sp^3 carbon is 328.41°. Our calculated primary KIE for the position of the transferring hydrogen of KIE = 1.07 is lower than experiment but consistent with an O_1-H_1 bond distance of 0.995 Å (MP2/6-31G* geometry).

The unsymmetrical approach of the peroxy acid to 1,3-butadiene (TS-**13**) and acrylonitrile (TS-**14**) that we predict on the basis of ab initio calculations is in excellent agreement with that proposed by Hanzlik on the basis of experimental KIE.[21] The unsymmetrical nature of TS-**13** (**a** and **b**) and TS-**14** (**a** and **b**) reflects the more polarizable nature of the carbon−carbon double bond of an α,*β*-unsaturated alkene.

The unsymmetrical nature of the transition state for styrene epoxidation is also most likely a reflection of extended conjunction with an aryl system. By contrast, the transition structure for a nonconjugated alkene exhibits a very soft potential energy surface for epoxidation and the final trajectory of the approaching peroxy acid will be determined to a large extent by steric factors. The observed stereospecificity of peroxy acid epoxidation reactions is also consistent with the transition states described herein since the rate of descent from transition structure to oxirane product for this concerted process must be orders of magnitude faster than C−C bond rotation in the absence of a discrete carbanionic intermediate.

4. Conclusions

(1) The epoxidations of propene and isobutene with peroxyformic acid proceed in a concerted way via slightly unsymmetrical Markovnikov-type transition structures where the differences in the bond distances between the double-bond carbons and the spiro oxygen are only 0.021 and 0.044 Å at the QCISD/6-31G* level. In contrast, the more polarizable nature of the carbon−carbon double bond of α,*β*-unsaturated systems results in a highly unsymmetrical transition structure for the epoxidation of 1,3-butadiene with an order of magnitude difference in the carbon−oxygen bond distances of 0.305 Å at the QCISD/6-31G* level. A highly unsymmetrical transition structure has been also found for the epoxidation of acrylonitrile.

(2) Notwithstanding the difference in the extent of asymmetry of the transition structures, both epoxidations of methyl-substituted alkenes and such α,*β*-unsaturated systems as 1,3-butadiene and acrylonitrile with peroxyformic acid follow a concerted asyncronous pathway. An unsymmetrical type of transition structure for 1,3-butadiene epoxidation and the concerted nature of the oxygen atom transfer step is consistent with the calculated kinetic isotope effects.

(3) Methyl substitution leads to a decrease in the epoxidation barriers from 18.8 kcal/mol for ethylene to 13.7 kcal/mol for isobutene at the QCISD(T)/6-31G*//QCISD/6-31G* level.

(4) While the activation barrier for the epoxidation of 1,3-butadiene with peroxyformic acid (15.9 and 11.7 kcal/mol at the QCISD(T)//QCISD and B3LYP levels, respectively) is close to that for propene epoxidation (16.0 and 12.0 kcal/mol at the QCISD(T)//QCISD/6-31G* and B3LYP/6-31G* levels, respectively), the barrier for acrylonitrile epoxidation is higher (21.0 and 17.3 kcal/mol at the QCISD(T)//QCISD/6-31G* and B3LYP/6-31G* levels, respectively). This increase in the barrier height reflects the decreased nucleophilicity of double bonds

bearing electron-withdrawing substituents. The closeness of the barriers for propene and 1,3-butadiene epoxidations supports the conclusion that both reactions have similar mechanisms albeit they differ in the asynchronous character of their transition structures.

(5) The epoxidation of 1,3-butadiene with peroxyformic acid is a more exothermic reaction ($\Delta H = -42.7$ kcal/mol using G2 theory) than the epoxidation of acrylonitrile (−40.5 kcal/mol). The former has a higher activation barrier than the latter. However, the difference in the reaction enthalpies (2.2 kcal/mol) is smaller than the difference in the activation barriers (5.1 kcal/mol).

(6) The energy differences between syn and anti configurations of the transition structures for the epoxidations of 1,3-butadiene and acrylonitrile with peroxyformic acid are very small (0.1−0.3 kcal/mol).

(7) A comparison of the barriers for alkene epoxidations calculated at the QCISD(T)/6-31G*//B3LYP/6-31G* level with the QCISD(T)/6-31G*//QCISD/6-31G* and CCSD(T)/6-31G*//QCISD barriers leads to the conclusion that using the B3LYP geometries in the QCISD(T) and CCSD(T) calculations can be cost effective and, at the same time, a reliable computational approach to study epoxidations of alkenes with peroxy acids.

Acknowledgment. This work has been supported by the National Science Foundation (CHE 96-96216). We are thankful to the National Center for Supercomputing Applications (Urbana, IL) and the Pittsburgh Supercomputing Center for generous amounts of computer time. Certain commercial materials and equipment are identified in this paper in order to specify procedures completely. In no case does such identification imply recommendation or endorsement by the National Institute of Standards and Technology, nor does it imply that the material or equipment identified is necessarily the best available for the purpose.

Supporting Information Available: G2 energies of formic acid, peroxyformic acid, and ethylene, propene, isobutene, 1,3-butadiene, and acrylonitrile as well as the epoxides of these alkenes (1 page, print/PDF). See any current masthead page for ordering information and Web access instructions.

JA980495G